Atmospheric Research 170 (2016) 112–122

Contents lists available at ScienceDirect

Atmospheric Research

journal homepage: www.elsevier.com/locate/atmosres

Chemical characterization and source apportionment of size-resolved particles in Hong Kong sub-urban area

Yuan Gao [a], Shun-Cheng Lee [a,*], Yu Huang [b], Judith C. Chow [b,c], John G. Watson [b,c]

[a] Department of Civil and Environmental Engineering, Research Institute for Sustainable Urban Development, The Hong Kong Polytechnic University, HungHom, Kowloon, Hong Kong
[b] Key Lab of Aerosol Chemistry & Physics, Institute of Earth Environment, Chinese Academy of Sciences, Xi'an 710075, China
[c] Division of Atmospheric Sciences, Desert Research Institute, 2215 Raggio Parkway, Reno, NV 89512, USA

ARTICLE INFO

Article history:
Received 21 July 2015
Received in revised form 26 October 2015
Accepted 26 November 2015
Available online 7 December 2015

Keywords:
Aerosol size distribution
Inorganic ions
Carbonaceous aerosol
MOUDI
PMF

ABSTRACT

Size-resolved particulate matter (PM) samples were collected with a 10-stage Micro-Orifice Uniform Deposit Impactor (MOUDI) at a sub-urban site (Tung Chung) in Hong Kong for four non-consecutive months representing four seasons from 2011 to 2012. Major chemical components were water-soluble anions (i.e., Cl^-, NO_3^-, and SO_4^{2-}), cations (i.e., NH_4^+, Na^+, K^+, and Ca^{2+}), organic and elemental carbon and elements. Both chemical mass closure and positive matrix factorization (PMF) were employed to understand the chemical composition, resolve particle size modes, and evaluate the PM sources. Tri-modal size distributions were found for PM mass and major chemical components (e.g., SO_4^{2-}, NH_4^+, and OC). Mass median aerodynamic diameters (MMADs) with similar standard deviations ($1.32 < \sigma < 1.42$) were 0.4, 0.7 and 3.8 μm, consistent with condensation, droplet and coarse modes. A bi-modal distribution peaking at condensation and droplet modes was found for EC, with a single mode peaking at 3.8 μm for Cl^-. Besides secondary SO_4^{2-}, carbonaceous aerosol dominated the condensation mode with 27% by engine exhaust and 18–19% each by residual oil combustion (shipping) and coal/biomass burning. Secondary SO_4^{2-} is also the most dominant component in the droplet mode, accounting for 23% of PM mass, followed by an industrial source (19%). Engine exhaust, secondary NO_3^-, and sea salt each accounted for 13–15% of PM mass. Sea salt and soil are the dominated sources in the coarse mode, accounting for ~80% of coarse mass.

1. Introduction

Airborne particulate matter (PM) scatters and absorbs sunlight, causing direct and indirect effects on Earth's radiation balance, visibility impairment, climate change, and human health (Penttinen et al., 2001; Seinfeld and Pandis, 2006; Watson, 2002). These effects are related to particle sizes and chemical compositions (Huang and Yu, 2008; Malm and Pitchford, 1997; Milford and Davidson, 1987; Sloane et al., 1991). Based on size-resolved measurements from a Micro-Orifice Uniform Deposition Impactor (MOUDI), Sloane (1983) and others quantified scattering efficiencies based on Mie theory (Sloane et al., 1991; Sloane and Wolff, 1985). Major chemical components (e.g., sulfate [SO_4^{2-}], nitrate [NO_3^-], and organics) have been used to understand the particle growth mechanisms as well as the physical and chemical characteristics (Howell and Huebert, 1998; Huang et al., 2006a; John et al., 1990; Kim et al., 2003; Plaza et al., 2011; Tang, 1996; Tsai et al., 2012; Wang et al., 2013).

Past studies in Hong Kong have showed high concentration for SO_4^{2-}, organic matter (OM), and elemental carbon (EC) in the submicron-mode, greatly influence local visual range and human health (Gao et al., 2015; Yao et al., 2002, 2003b; Zhuang et al., 1999b), similar to observations from other countries (John et al., 1990; Kim et al., 2003; Plaza et al., 2011). Chow et al. (2008) observed a SO_4^{2-} size distribution that was multi-modal and wider at an urban site than the uni-modal distribution found at a rural site in central California. Bian et al (2014) found significant size distribution changes over the past 20 year periods when compared with the three inorganic compounds (i.e., SO_4^{2-}, NO_3^-, and NH_4^+) at the same site. $PM_{2.5}$ or PM_{10} source apportionment studies have been conducted in Hong Kong via different receptor models (Fung and Wong, 1995; Guo et al., 2009; Lee et al., 1999), e.g. Multivariate Regression Analysis, Principal Component Analysis with Absolute Principal Component Scores technique (PCA-APCS), Chemical Mass Balance (CMB), and Positive Matrix Factorization (PMF), finding contributions from engine exhaust, secondary aerosols, residual oil combustion, fresh and aged sea salt, soil, coal combustion and biomass burning. Only few source apportionment studies investigated have examined contribution to different size ranges (Contini et al., 2014; Han et al., 2006; Kim et al., 2003), but not in Hong Kong.

* Corresponding author. Tel.: +852 2766 6011; fax: +852 2334 6389.
E-mail address: ceslee@polyu.edu.hk (S.-C. Lee).

http://dx.doi.org/10.1016/j.atmosres.2015.11.015
0169-8095/

The Tung Chung (TC) site is a newly developed sub-urban area in Hong Kong, located in the centerline of the Pearl River Delta (PRD) region. It is a gateway to Macau and mainland China, with ~78,400 inhabitants (*2011 Census*) and increasing industrial and commercial activities, such as coal-fired power plants, airports, seaports, and local traffic (Wang et al., 2005; Zhou et al., 2014). Therefore, it is essential to understand the air pollution in this area.

The objectives of this study are to: 1) investigate the particle size distribution of water-soluble ions and carbon; and 2) determine resolved size mode and source apportionment by the Positive Matrix Factorization (PMF) receptor model applied to MOUDI (Model 110, MSP Corp. Minnesota, U.S.A.) data.

2. Methods

2.1. Sampling site and sampling periods

The TC site (22.17 °N, 113.56 °E) is on the northern coast of Lantau Island and southwest of Hong Kong (Fig. 1). It is a new town area, ~3 km from the Hong Kong International Airport. MOUDI samplers were placed on a three story building which was established by Hong Kong Environmental Protection Department (HKEPD). Sampling was conducted for 27 days and covers four periods: August/September (2011), November/December (2011), February/March (2012), and May (2012), representing summer, fall, winter, and spring seasons, respectively. Sample duration was 24 h, from 10:00 a.m. to 10:00 a.m. the next day local standard time (LST). Table 1 details the sampling dates and daily meteorological conditions.

2.2. Size-resolved particle measurements

The ten-stage MOUDI includes the following aerodynamic particle diameter ranges with 30 L/min flow rate: 0.056–0.1, 0.1–0.18, 0.18–0.32, 0.32–0.56, 0.56–1.0, 1.0–1.8, 1.8–3.2, 3.2–5.6, 5.6–10, and 10–18 μm. One MOUDI contained 47 mm Teflon-membranes Filters (Pall Sciences, New York, U.S.A.) and another contained 47 mm quartz-fiber filters (QMA, Whatman, Maidtone, England) as substrates. Backup filters were 37 mm. The spacer (0.05 in. in thickness) provided by MSP Corp. (MN, U.S.A.) was placed between adjacent stages to compensate for the lower jet-to-plate distance caused by the filter thickness (Huang et al., 2006b; Bian et al., 2014). Fujitani et al. (2006) reported that quartz-fiber filter artifacts are minimal compared with aluminum foils or Teflon-membrane filter for PM concentrations of ~42 μg/m^3.

Ions and carbon were analyzed on quartz-fiber filters with mass and elements analyzed on Teflon-membrane filters. During the sampling periods, the effect of particle bounce should be negligible since the relative humidity (RH) was high, ~60% to 80% (Chow et al., 2005; Huang et al., 2004; Milford and Davidson, 1987).

Before sampling, quartz-fiber filters were prefired at 900 °C for 3 h to minimize organic artifacts (Chow et al., 2010a; Ho et al., 2006; Watson et al., 2009). Both the Teflon-membrane and quartz-fiber filters were weighed before and after sampling, using a microbalance (Model MC5, Sartorius, Goettingen, Germany) with a sensitivity of ±1 μg in the 0–250 mg range. Before weighing, filters were equilibrated in a desiccator for 24 h at temperature (25 ± 5 °C) and RH (35 ± 10%) controlled environment. After weighing, filters were stored air-tight in a refrigerator (<4 °C) to minimize evaporation of volatile components. Sample flow rates within ±10% of the specification were verified at the beginning and end of each sampling period.

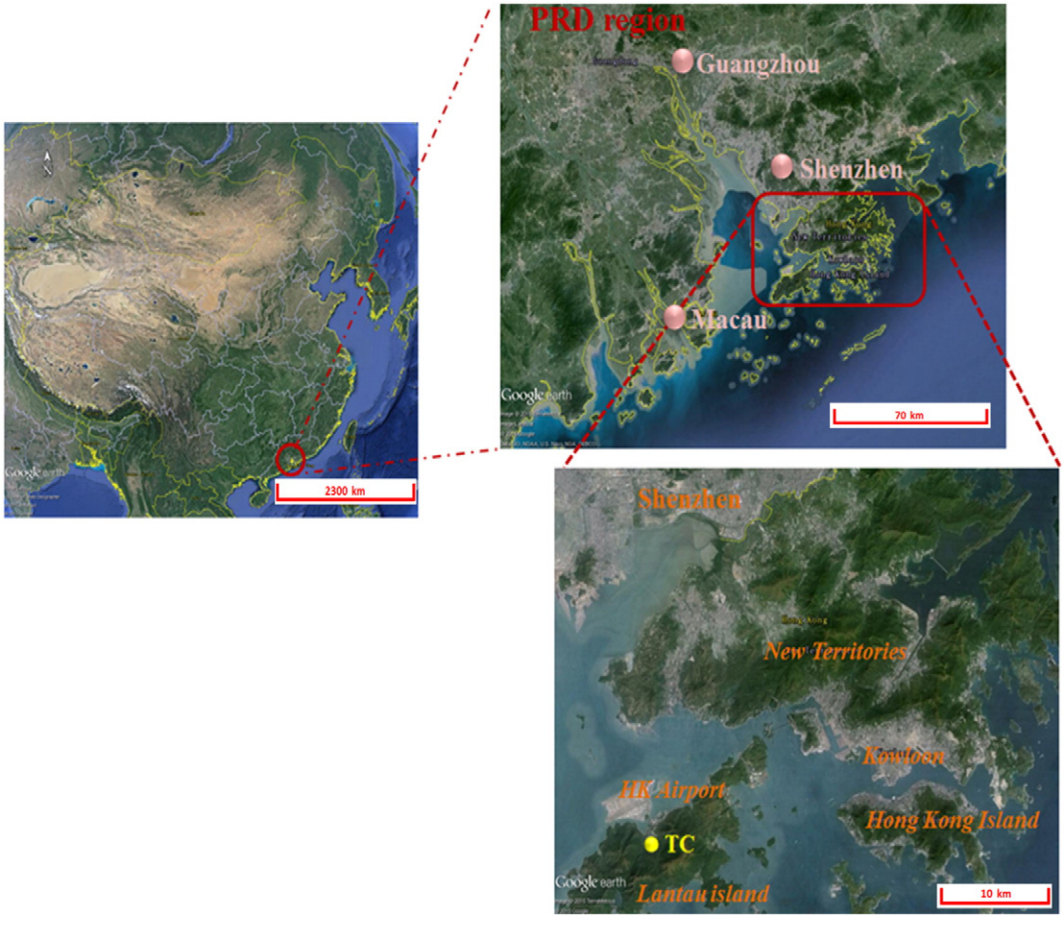

Fig. 1. Location of sampling site, at the Tung Chung monitoring station (TC), Hong Kong.

Table 1
Meteorological characteristics during each sampling dates.

Seasons	Sampling date	Prevail wind[a]	Wind speed (m/s)	Temperature (°C)	Relative humidity %
August/September (summer), 2011	August 4th–5th, 2011	SW	11.40	32	69
	August 22nd–23rd, 2011	SW	11.20	32	71
	August 24th–25th, 2011	NE	11.20	32	72
	August 29th–30th, 2011	NW	16.20	34	64
	September 6th–7th, 2011	SE	12.70	32	71
	September 8th–9th, 2011 (blank)	SE	6.38	30	76
November/December (fall), 2011	November 3rd–4th, 2011	NE	6.04	28	68
	November 8th–9th, 2011	NE	10.63	22	80
	November 14th–15th, 2011	NE	8.85	25	68
	November 21st–22nd, 2011	NE	10.04	22	60
	November 25th–26th, 2011	NE	10.6	22	60
	December 1st–2nd, 2011	N	9.56	16	57
	December 3rd–4th, 2011 (blank)	N	7.74	18	80
February/March (winter), 2012	February 2nd–3rd, 2012	NE	8.89	16	70
	February 9th–10th, 2012	E	8.92	14	79
	February 15th–16th, 2012	NE	5.08	20	85
	February 20th–21st, 2012	NE	10.01	18	66
	February 27th–28th, 2012	NE	7.97	10	80
	March 2nd–3rd, 2012	NE	5.16	22	83
	March 4th–5th, 2012 (blank)	NE	6.36	18	89
May (spring), 2012	May 2nd–3rd, 2012	SW	7.83	30	74
	May 9th–10th, 2012	SW	6.86	31	69
	May 14th–15th, 2012	SE	3.11	30	75
	May 21st–22nd, 2012	SE	11.52	27	67
	May 24th–25th, 2012	E	8.33	28	75
	May 30th–31st, 2012	E	6.08	29	75
	June 1st–2nd, 2012 (blank)	SE	10.36	27	82

[a]Refer to prevail wind direction, N—North, NE—Northeast, E—East, SE—Southeast, S—South, SW—Southwest, W—West, NW—Northwest.

2.3. Chemical analysis

After gravimetric analyses, Teflon-membrane filters were analyzed for 51 elements (from Na to U) at the Institute of Earth and Environment, Chinese Academy of Science, China, by energy-dispersive X-Ray Fluorescence (XRF) analyses (Epsilon 5 ED-XRF, PANalytical B. V., the Netherlands, Watson et al., 1999). The quartz-fiber filters were analyzed for carbon fractions and water-soluble ions at the Air Laboratory of the Hong Kong Polytechnic University (HKPU). A punch from each quartz-fiber filter (0.526 cm^2) was used for organic and elemental carbon (OC and EC) analysis using a DRI Model 2001 Thermal/Optical Carbon Analyzer (Atmoslytic Inc, Calabasas, CA, USA), following the IMPROVE_A-thermal/optical reflectance (TOR) protocol (Chow et al., 2007, 2011). For ion analysis, half of each quartz-fiber filter was extracted in 10 mL of ultra-pure deionized distilled water (specific resistance ≥18.1 MΩ, Millipore). Extraction solutions were filtered and stored in plastic vials in a refrigerator (<4 °C) until analysis. Water soluble ions including chloride (Cl^-), nitrate (NO_3^-), sulfate (SO_4^{2-}), sodium (Na^+), potassium (K^+), calcium (Ca^{2+}), and ammonium (NH_4^+) were analyzed by ion chromatography (ICS3000, DIONEX, Sunnylvale, C.A., U.S.A.) (Chow and Watson, 1999).

Reconstructed mass equation by chemical mass closure method, including soil, inorganic ions (i.e., SO_4^{2-}, NO_3^-, and NH_4^+), a biomass burning marker (K^+), EC, OM, trace element oxides (TEO) and sea salt

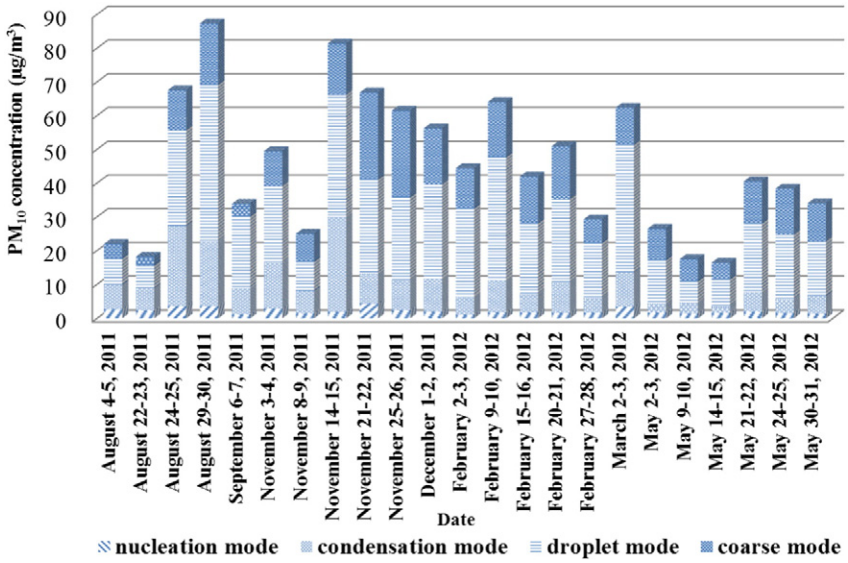

Fig. 2. Time series of PM_{10} concentrations (particle size modes are defined as: 0.056–0.1 μm for nucleation mode, 0.1–0.56 μm for condensation mode, 0.56–1.8 μm for droplet mode, and 1.8–10 μm coarse mode).

Table 2
Seasonal $PM_{1.8}$ and PM_{10} concentrations in Tung Chung, Hong Kong.

Seasons (N = 23)	$PM_{1.8}$ μg/m^3	PM_{10} μg/m^3	$PM_{1.8}/PM_{10}$
August/September (summer), 2011			
Clean day	19 ± 8	23 ± 7	0.83 ± 0.02
Episode day	62 ± 8	80 ± 13	0.78 ± 0.04
Average	38 ± 20	47 ± 27	0.81 ± 0.06
November/December (fall), 2011			
Average	37 ± 13	53 ± 17	0.70 ± 0.09
February/March (winter), 2012			
Average	34 ± 11	48 ± 11	0.71 ± 0.08
May (spring), 2012			
Average	26 ± 7	39 ± 11	0.66 ± 0.03

(Chow et al., 2010b, 2015; Kong et al., 2014; Kumar et al., 2008; Malm et al., 1994; Sisler et al., 1996; Zhang et al., 2013) as follows:

$$\text{Soil} = 2.2 \times \text{Al} + 2.49 \times \text{Si} + 1.63 \times \text{Ca} + 2.42 \times \text{Fe} + 1.94 \times \text{Ti} \quad (1)$$

Malm et al., 1994

$$\text{Particulate organic matters (POM)} = 1.8 \times \text{OC} \quad (2)$$

(Hand et al., 2011)

$$\text{Trace element oxide (TEO)} = 1.3 \times [0.5 \times (\text{Sr} + \text{Ba} + \text{Mn} + \text{Co} + \text{Rb} + \text{Ni} + \text{V}) + 1.0 \times (\text{Cu} + \text{Zn} + \text{Mo} + \text{Cd} + \text{Sn} + \text{Sb} + \text{Tl} + \text{Pb} + \text{As} + \text{Se} + \text{Ge} + \text{Cs} + \text{Ga})] \quad (3)$$

(Zhang et al., 2013)

$$\text{Sea salt} = 1.47 \times \text{Na}^+ + \text{Cl}^- \quad (4)$$

(Kong et al., 2014)

2.4. PMF model

Positive matrix factorization (PMF) model version 3.0 was used to resolve different size modes and identify potential sources. Many previous studies have successfully applied this factor analysis method to resolve the overlapping peaks (Guo et al., 2010; Huang et al., 2006c; Kim et al., 2003). MOUDI size distribution data was viewed to be data matrix X of sample i by j dimensions:

$$X_{ij} = \sum_{k=1}^{p} g_{ik} f_{kj} + e_{ij} \quad (5)$$

where i is the number of the samples, and j is the MOUDI stages (or chemical species). Total factors p would be the resolved modes, g_{ik} is mass contribution of each factor k to the individual sample i, f_{kj} is the species profile j of each source factor k, and e_{ij} is the residual for each sample i or species j.

The measured chemical species concentration and their equation-based uncertainty files should input into the model for further analysis. Detailed calculation method for chemical species uncertainties is explained in the PMF user's manual and by Tan et al. (2014, 2016). When a species concentration is below detection limits for more than 50% of the samples, that species is excluded (Yau et al., 2013). Chemical species were categorized as "strong", "weak", and "bad" (Paatero and Tapper, 1994; Watson et al., 2015). S/N ratios >2 were categorized as "strong" and ratios between 0.2 and 2 were categorized as "weak". S/N ratios <0.2 were assigned to the "bad" category and were excluded in the PMF analysis.

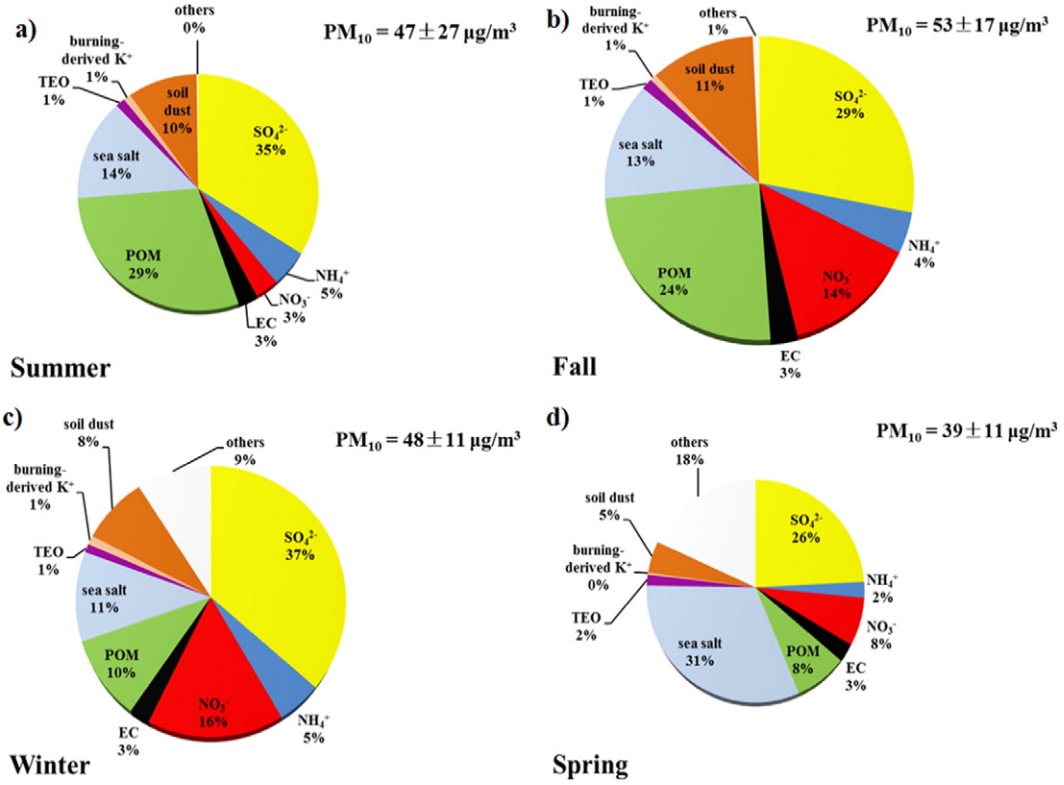

Fig. 3. Reconstructed PM_{10} mass for: a) summer, b) fall, c) winter and d) spring. The components include, sulfate, nitrate, ammonium, Particulate organic matters ($POM = 1.8 \times OC$), EC, water-soluble potassium, trace element oxides ($TEO = 1.3 \times [0.5 \times (\text{Sr} + \text{Ba} + \text{Mn} + \text{Co} + \text{Rb} + \text{Ni} + \text{V}) + 1.0 \times (\text{Cu} + \text{Zn} + \text{Mo} + \text{Cd} + \text{Sn} + \text{Sb} + \text{Tl} + \text{Pb} + \text{As} + \text{Se} + \text{Ge} + \text{Cs} + \text{Ga})]$, sea salt($sea\,salt = 1.47 \times \text{Na}^+ + \text{Cl}^-$), soil($soil = 2.20 \times \text{Al} + 2.49 \times \text{Si} + 1.63 \times \text{Ca} + 2.42 \times \text{Fe} + 1.94 \times \text{Ti}$).

The number of factors should represent the actual sources situation, although there are sources mixing within factors. The Q value used to determine how well the factors and contributions reproduce the input, which should approximately equal the number of freedom degree or approximately equal to the data points in the data group (Polissar et al., 1998; Yau et al., 2013; Tan et al., 2014).

3. Results and discussion

3.1. Particle mass and major chemical compositions

Temporal variations of PM mass concentrations in Fig. 2, show large day-to-day variations with higher concentration found during fall and winter. The droplet mode (0.56–1.8 μm) shows the largest contribution, accounting for 27–59% of PM_{10} mass, followed by the condensation mode (0.1–0.56 μm) and coarse modes (1.8–10 μm) in the range of 10–42% and 10–34% of PM_{10}, respectively. Table 2 summarizes daily average $PM_{1.8}$ and PM_{10} concentrations for the four seasons. Seasonal average $PM_{1.8}$ and PM_{10} varied from 26 and 39 μg/m^3 in spring to 37 and 53 μg/m^3 in fall, respectively. The highest average concentration (80 ± 13 μg/m^3) was found during summer hazy days, with a $PM_{1.8}$/PM_{10} ratio of 0.78 ± 0.04. As shown in Table 2, both $PM_{1.8}$ and PM_{10} concentrations increased by 3–4 fold during pollution episodes, but the ratio of $PM_{1.8}$ to PM_{10} decreased from 0.83 ± 0.02 (clean days) to 0.78 ± 0.04 (episode days), indicating increasing particle sizes for the polluted days. Approximately 39% of samples exceeded the 24-hour PM_{10} standard/guideline of 50 μg/m^3 in Europe and WHO. $PM_{1.8}$ and PM_{10} concentrations were ~20–60% lower than those at urban sites in Hong Kong (Chow et al., 2010b; Ho et al., 2006; Louie et al., 2005). Comparable $PM_{2.5}$ concentrations were found at the Tai'O (41 μg/m^3) and Tung Chung (37 μg/m^3) sites (Cheung et al., 2005), with fine particle to PM_{10} ratios averaging 0.72 ± 0.09, and ranging from 0.46 to 0.88.

The reconstructed PM_{10} mass for each season in Fig. 3 shows a high correlation (R = 0.8–0.97) with gravimetric PM_{10} mass. SO_4^{2-} is the most abundant species, accounting for 26–37% of PM_{10} mass. POM is the second largest component, constituting 8–10% of PM_{10} during spring and winter to 24–29% during fall and summer. NO_3^- accounts for 14–16% of PM_{10} in fall and winter, reduced to ~8% in spring and ~3% in summer. Some NO_3^- maybe volatized during warm seasons. Sea salt contributed its largest fraction in spring (~31%) and was lowest in winter (11%). Sea salt fractions of PM_{10} during summer and fall were ~14%. Soil contribution ranged from 5% in spring to 10–11% in summer and fall. There are no apparent seasonal variations for NH_4^+ (2–5%), EC (5%), TEO (1–2%), and K^+ (0–1%). Differences between reconstructed and measured PM_{10} (i.e., others) were higher in winter and spring (9–18%), which could be attributed to sampling and analysis uncertainties (Chow et al, 2015).

3.2. Resolved particle size distribution modes

PMF has been used to resolve particle size distributions by Garrido Frenich et al. (2000), Huang et al. (2006a, 2006c), Kim et al. (2003) and Yu et al. (2010). The nucleation, condensation, droplet, and coarse modes, indicate PM origins and aging. Droplet mode particles form

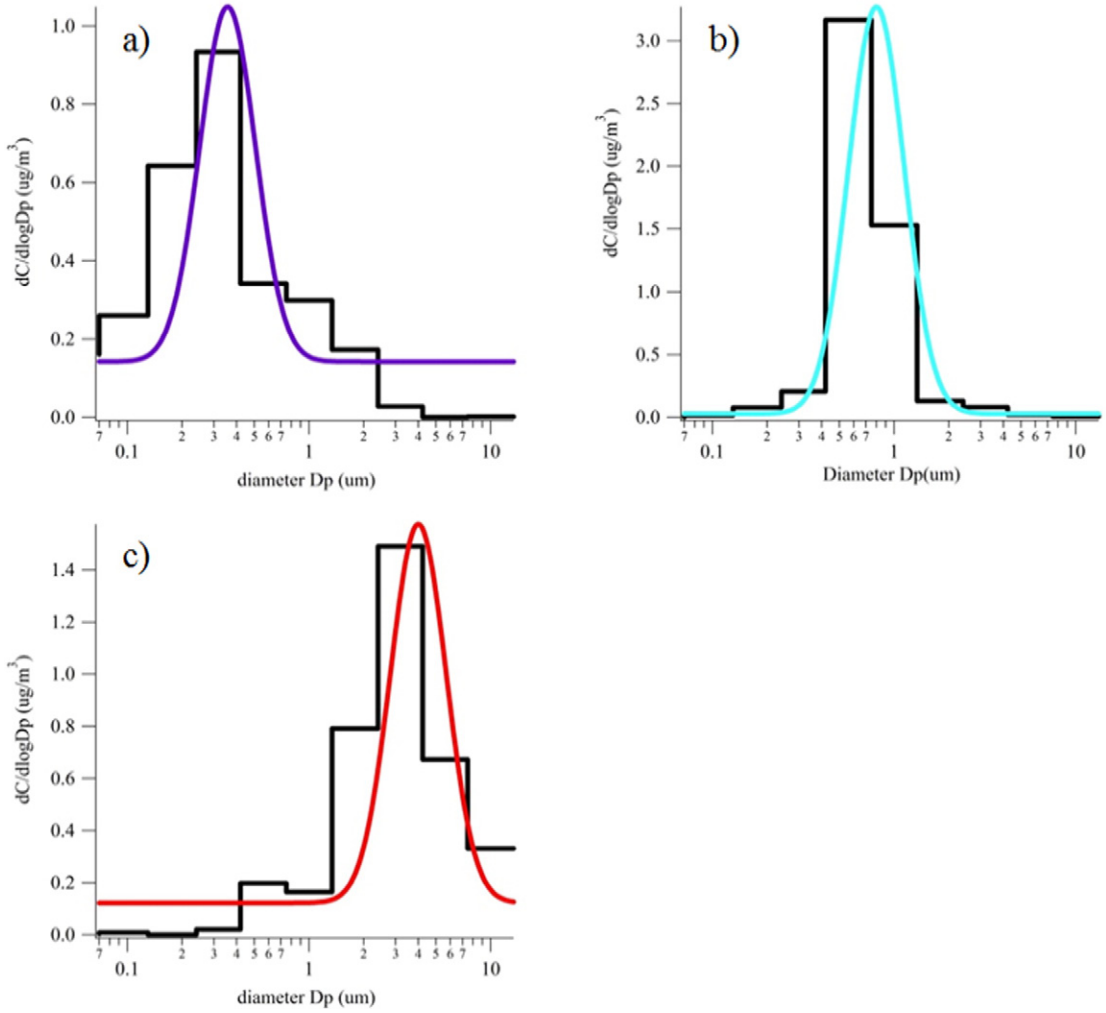

Fig. 4. Resolved particle mass size distributions for: a) condensation mode, b) droplet mode, and c) coarse mode in PMF.

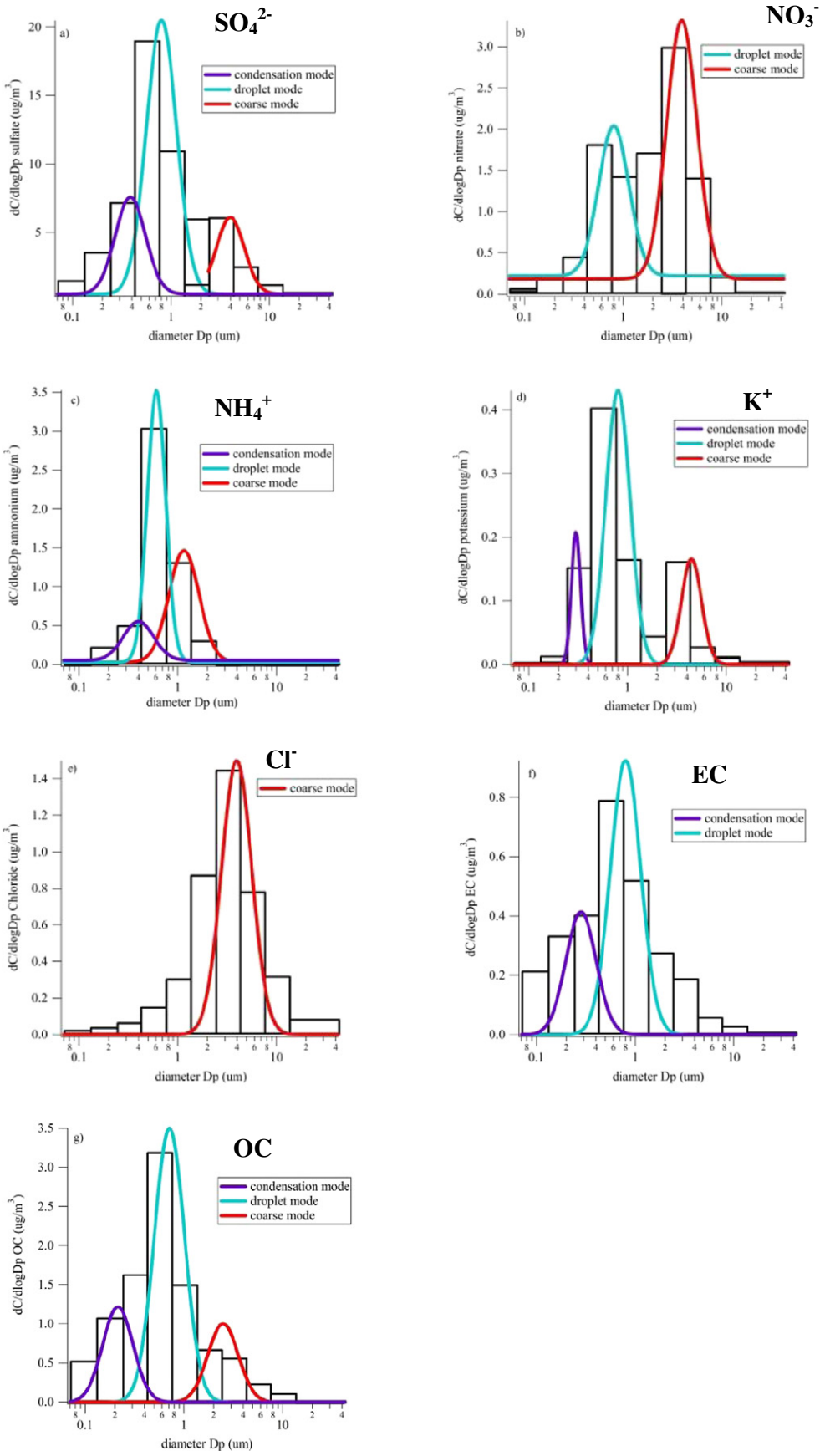

Fig. 5. Average size distributions for: a) sulfate, b) nitrate, c) ammonium, d) water-soluble potassium, e) chloride, f) EC, and g) OC.

through aqueous reaction in clouds and fogs (Hering and Friedlander, 1967; Seinfeld and Pandis, 2006). A total of 161 samples (23 sets × 7 species (i.e., ions and carbon)) and their equation-based uncertainties were used in PMF 3.0 software, with typical results shown in Fig. 4. Mass median aerodynamic diameter (MMAD) and standard deviation (σ) were 0.4 μm (σ = 1.42), 0.7 μm (σ = 1.32), and 3.8 μm (σ = 1.38), respectively. The standard deviation (σ) illustrates the width of distribution; a lower σ value indicates narrower distribution. Similar MMADs and σ for condensation (0.34 ± 1.39 μm) and droplet (0.84 ± 1.39 μm) modes were observed in urban Shenzhen and Beijing, but the coarse mode MMADs were higher than those at TC, 5.4 ± 1.56 μm and 5.7 ± 1.39 μm, respectively (Guo et al., 2010; Lan et al., 2011).

Fig. 5 shows resolved size distributions for 7 species (i.e., SO_4^{2-}, NO_3^-, NH_4^+, Cl^-, K^+, OC, and EC). Tri-modal size distributions were found for SO_4^{2-}, with one dominated peak in the droplet mode (0.8 μm, σ = 1.2), and small peaks for the condensation and coarse modes (Fig. 5a). The SO_4^{2-} size distribution is consistent with: 1) a condensation mode formed by gas-to-particle conversion (e.g., photochemical oxidation of sulfur dioxide (SO_2) (Lan et al., 2011; Seinfeld and Pandis, 2006); 2) a droplet mode formed by aqueous SO_2 oxidation (John et al., 1990; Kerminen and Wexler, 1995; Zhuang et al., 1999b); and 3) a coarse mode formed by reactions with sea salt or soil (Zhuang et al., 1999a). The resolved SO_4^{2-} size distribution is similar to previous studies in Hong Kong and mainland China (Guo et al., 2010; Lan et al., 2011; Yao et al., 2003a; Zhuang et al., 1999b), attributing ~60% of SO_4^{2-} to in-cloud process, ~25% to gas-phase chemistry, and ~15% to reactions with soil and sea salt (R = 0.8, between Na^+ and SO_4^{2-}, in summer and fall).

In-cloud process and condensation onto pre-existing particles are also the potential pathways to form droplet and condensation NO_3^-. Thermodynamic equilibrium state is the dominant factor that affects NO_3^- size distribution (John et al., 1990; Seinfeld and Pandis, 2006), where:

$$HNO_3(g) + NH_3(g) \leftrightarrow NH_4NO_3(s, aq). \quad (6)$$

When the gaseous ammonia (NH_3) and nitric acid (HNO_3) are larger than the equilibrium constant, the ammonium nitrate (NH_4NO_3) will be presented (Zhuang et al., 1999b). Fig. 5b shows abundant coarse mode (~67% of NO_3^-), followed by droplet mode (~33%). Coarse mode NO_3^- results from the reaction of nitric acid (HNO_3) with alkaline sea salt and soil. Fine particle NO_3^- is semi-volatile and changes between gas and particle phases depending on ambient temperature and RH (Chow et al., 2008). This may explain why only a few condensation mode peaks were observed in this study.

SO_4^{2-} and NO_3^- contribution can be elucidated by the sulfur oxidation ratio (SOR) and the nitrogen oxidation ratio (NOR):

$$SOR = \frac{[SO_4^{2-}]}{[SO_4^{2-} + SO_2]} \quad (7)$$

$$NOR = \frac{[NO_3^-]}{[NO_3^- + NO_2]}, \quad (8)$$

where SO_4^{2-}, sulfur dioxide (SO_2), NO_3^-, and nitrogen dioxide (NO_2) are molar concentrations in units of mol/m^3. Higher SOR and NOR values indicate that larger amounts of secondary SO_4^{2-} and NO_3^- particles were formed by photochemical oxidation of precursor gases (Kadowaki, 1986; Khoder, 2002). Fig. 6 shows the SORs and NORs for three size modes. The NORs are lower than SORs in spring and summer and higher in fall and winter, implying different SO_4^{2-} and NO_3^- formation and removal mechanisms. The seasonal pattern for SORs was opposite that for NORs. Higher temperatures in summer and spring (23–29 °C) favor the formation of SO_4^{2-} by photochemical oxidation, but these

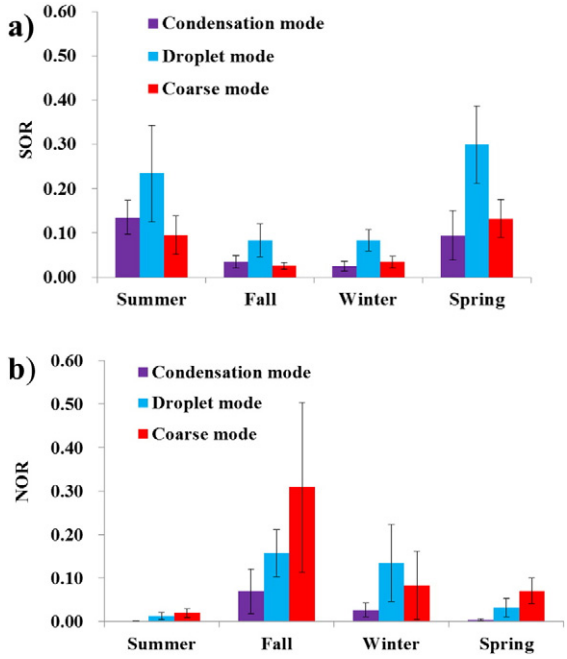

Fig. 6. Size-fractionated: a) sulfur oxidation ratio (SOR); and b) nitrogen oxidation ratio (NOR) in four seasons.

enhance the volatilization of NO_3^-. Correlations between SOR and temperature increase as particle size decreases. SOR is the highest for the droplet mode, ~60% higher than for the condensation and coarse modes. NOR is most abundant in the coarse mode as compared to condensation and droplet modes, suggesting the sea salt or soil formation of coarse particle NO_3^- (e.g., sodium nitrate and calcium nitrate). Reasonable correlation (R = 0.6) was found between RH and NOR, suggesting aqueous phase reactions under high RHs.

NH_4^+ and K^+ are mostly in the droplet mode (Fig. 5c and d). The molar ratio of NH_4^+ to SO_4^{2-} in fine mode was 1.0, indicating incomplete neutralization of ammonium bisulfate and sulfuric acid (Liu et al., 2008). A similar K^+ size distribution was found in Shenzhen and PRD region (Andreas, 1983; Huang et al., 2006a; Lan et al., 2011; Novakov and Corrigan, 1996). Small peak of K^+ in coarse mode may due to coagulation process of biomass burning emissions from small particles and sea salt (Bian et al., 2014). A single coarse mode was found for Cl^- (Fig. 5e), indicative of the presence of sea salt, similar to that found by Yao et al. (2003b).

EC in the condensation (0.28 μm) and droplet (0.8 μm) modes contributed 0.5 and 0.6 μg/m^3, respectively, consistent with fresh and slightly aged engine exhaust, similar to those found in Shenzhen (Huang and Yu, 2008). Dominated droplet mode in EC suggests aged EC which nucleated and condensed from fresh EC emissions. Some correlation was found between EC and SO_4^{2-} (R = 0.72), may be related to fuel sulfur contents, especially from heavy oils used in ocean-going vessels. Previous studies in PRD region suggested internal mixed of EC and SO_4^{2-} and aqueous processes (Cheng et al., 2006; Huang and Yu, 2008). Abundance of droplet mode was also apparent for OC, followed by condensation mode. OC concentrations in the condensation, droplet, and coarse modes are 1.9, 2.0 and 0.4 μg/m^3, respectively. The OC/EC ratios are >2 in the droplet and condensation modes.

3.3. Pollution episodes

There was one polluted episode occurred during summer, including one clean day, on August 20th to 21st and two polluted days representing the beginning (August 24th to 25th) and ending (August 29th to 30th) of the pollution episode (Fig. 7a). The ratio of each particle size mode to PM_{10} changes significantly from clean day to the end of

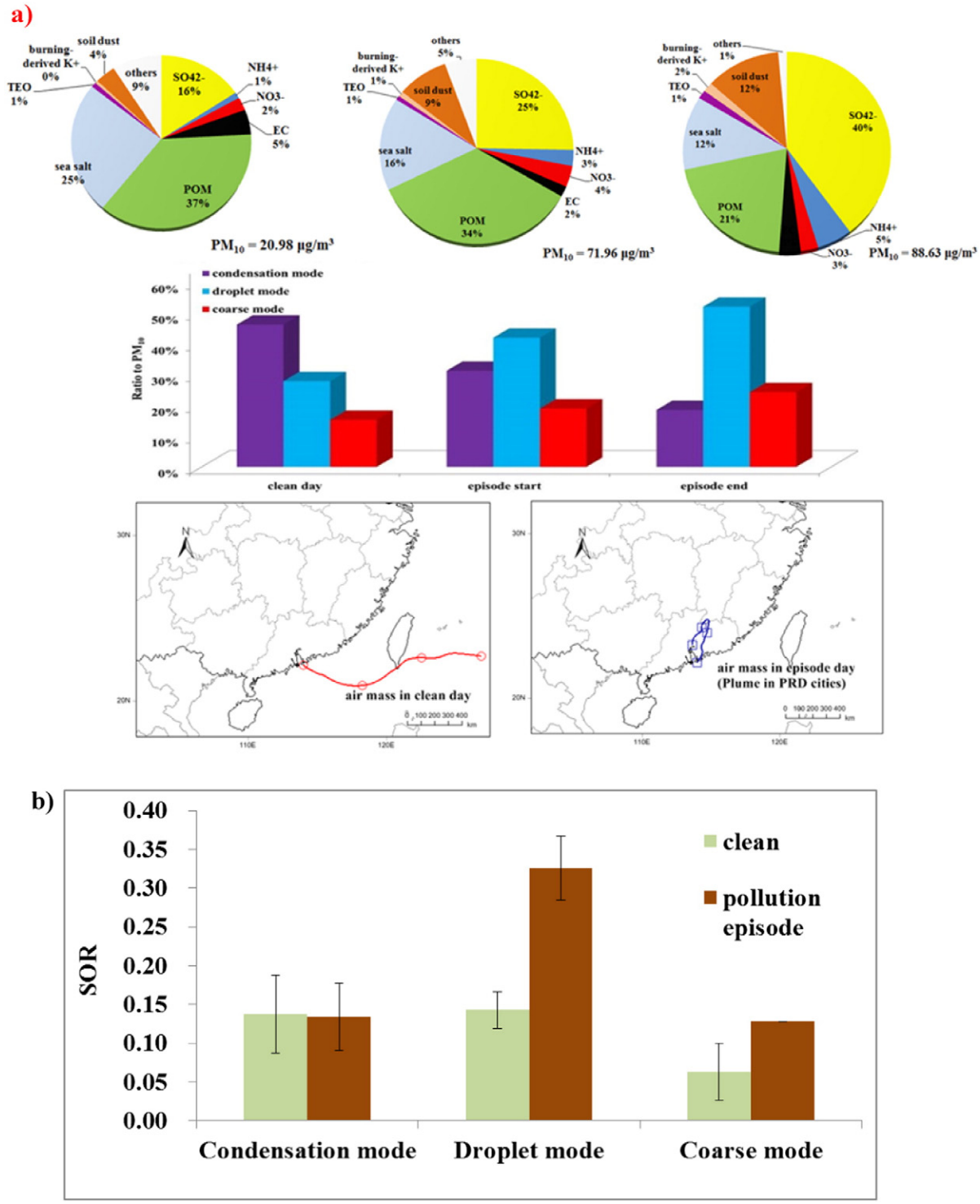

Fig. 7. a) Reconstructed PM mass clean (20.98 μg/m^3) on August 20th, starting episode (71.96 μg/m^3) on August 24th, and ending episode (88.63 μg/m^3) on August 29th; abundances of each particle size modes in PM_{10} and air trajectory patterns are also shown; and b) size-fractionated SOR value in clean and episode days.

pollution episode day. On the polluted days, particles in the condensation mode decreased from ~31% to ~18%, with concurrent increases in the droplet mode from ~42% to 52%, and a partial increase (~19% to 24%) in the coarse mode. Chemical mass closure also showed major chemical components have significant differences. PM_{10} fraction of POM and EC for clean and episode ending days, reduced from 36% to 24%, suggesting a larger regional-scale contribution. The abundance of SO_4^{2-} in PM_{10} increased from 16% to 40%, showing secondary aerosol formation process dominated the episode period. Back trajectories were used to identify the origin of the sources during the clean and episode days. As shown in Fig. 7a, the clean day air mass originated from the ocean, bringing uncontaminated air to the TC. During the episode, polluted and stagnant air masses come from the PRD region.

The mass ratio of nonseasalt-SO_4^{2-} (i.e., SO_4^{2-}–0.253 × Na^+) and NO_3^- can be used to indicate contribution acidity (Kong et al., 2014). The ratios of NSS-SO_4^{2-} and NO_3^- were increased significantly, from 2.3, 19, to 36 for clean, episode starting and episode ending days, respectively. Particle acidity during this episode period is more affected by

Table 3
Fraction of PM source factors in each size mode.

Sources	Source makers	Condensation mode (0.1–0.56 μm)	Droplet mode (0.56–1.8 μm)	Coarse mode (1.8–10 μm)
Residual oil combustion	V	21%	N.A.	N.A.
Engine exhaust	EC, OC	26%	14%	N.A.
Coal/biomass burning	As, Pb, K^+	16%	2%	N.A.
Secondary sulfate	NH_4^+, SO_4^{2-}	37%	24%	N.A.
Secondary nitrate	NO_3^-, K^+	N.A.	13%	N.A.
Incineration	Cu, Zn, OC	N.A.	6%	N.A.
Industry	Mn, Cs	N.A.	19%	19%
Sea salt	Cl, Na, Mg	N.A.	15%	52%
Soil	Si, Al, Fe, Ti, Ca, Fe	N.A.	7%	29%

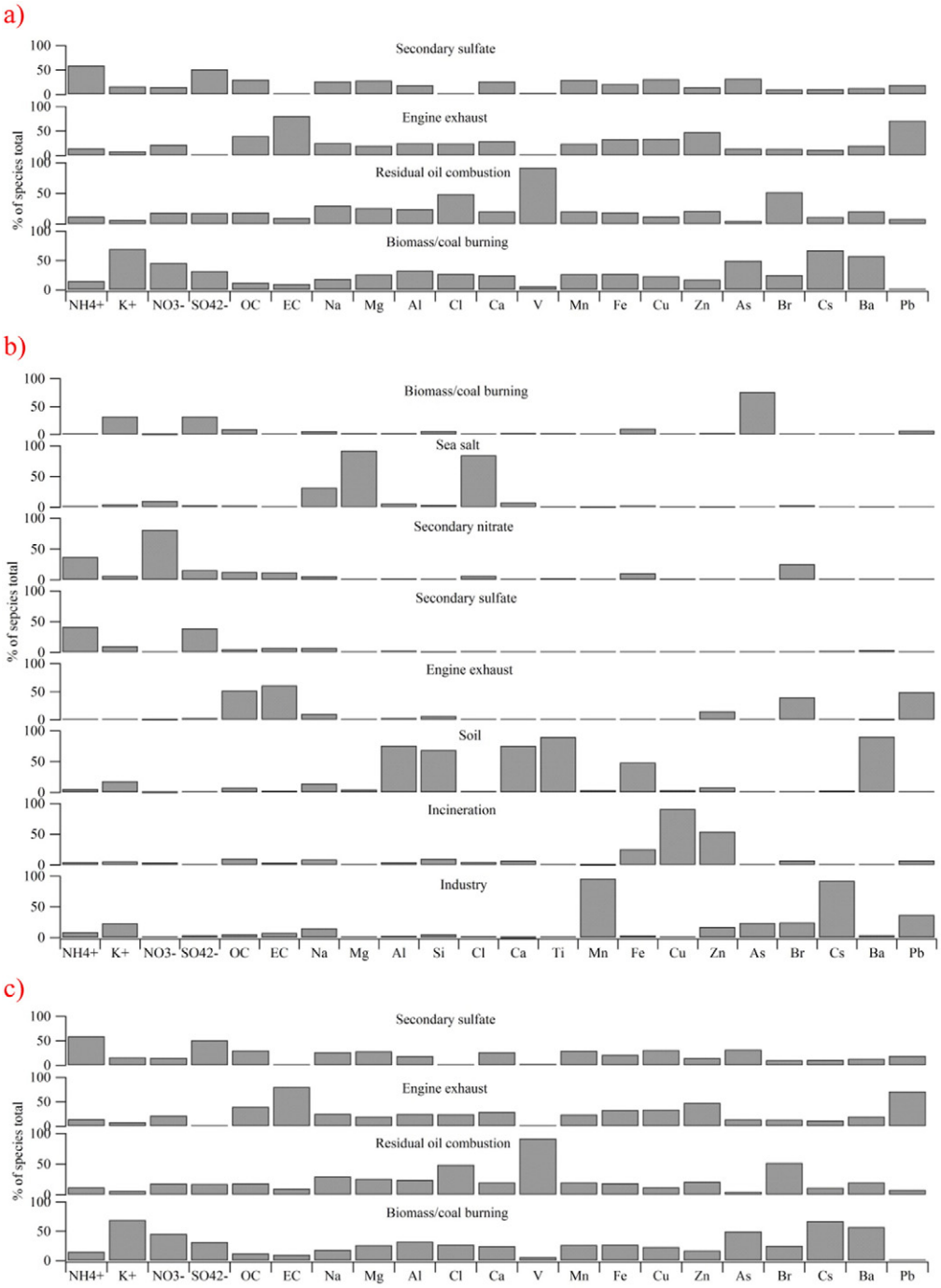

Fig. 8. Source factors for: a) condensation, b) droplet, and c) coarse mode; chemical species in condensation mode for PMF are NH_4^+, K^+, NO_3^-, SO_4^{2-}, OC, EC, Na, Mg, Al, Cl, Ca, V, Mn, Fe, Cu, Zn, As, Br, Cs, Ba and Pb. The chemical species in droplet mode contains NH_4^+, K^+, NO_3^-, SO_4^{2-}, OC, EC, Na, Mg, Al, Si, Cl, Ca, Ti, Mn, Fe, Cu, Zn, As, Br, Cs, Ba and Pb. In addition, chemical species in coarse mode are NH_4^+, K^+, NO_3^-, SO_4^{2-}, OC, EC, Na, Mg, Al, Si, Cl, Ca, Ti, Mn, Fe, Cu, Zn, Cs, Ba and Pb.

SO_4^{2-} than NO_3^- (Kong et al., 2014). Fig. 7b shows a remarkable high SOR value in the droplet mode during the polluted days. Due to high temperature in summer, the NOR did not exhibit much change.

3.4. Source factors in condensation, droplet, and coarse modes

Source apportionment by PMF 3.0 software was conducted for the three size modes (i.e., condensation, droplet and coarse modes). A total of 69 (23 sets × 3 stages) filter samples with their measured chemical species concentrations and associated uncertainties were input into the model (Huang et al., 2006b). Table 3 and Fig. 8 summarize the nine source factors and their identified markers (Choi et al., 2001; Han et al., 2006; Senaratne and Shooter, 2004; Tan et al., 2014, 2016; Yau et al., 2013). Similar to mass size distribution pattern in Fig. 4, eight source factors were found for the droplet mode, four source factors for the condensation mode, and three for the coarse mode, as shown in Fig. 9. Sea salt and soil factors contributed >80% of the coarse mass. Anthropogenic sources contributed to the droplet mode, with 24% from the secondary SO_4^{2-} factor, 19% from the industrial emissions factor and 13–15% each from the engine exhaust, secondary NO_3^-, and sea salt factors. Other source factors contributed 10% of the droplet mode particle mass concentrations. The condensation mode had 37% contribution from the secondary SO_4^{2-} factor, 27% from the engine exhaust factor, and 18–19% each from the residual oil combustion and coal/biomass burning factors.

4. Conclusions

Size-segregated samples were collected by 10-stage Micro-Orifice Uniform Deposit Impactor (MOUDI) for the four seasons: summer (August/September, 2011), fall (November/December, 2011), winter (February/March, 2012), and summer (May, 2012). In addition to gravimetric mass, water-soluble ions, organic/elemental carbon, and elemental species were analyzed. The major chemical components were examined using chemical mass closure method. The size distribution of major chemical species and source apportionment on size-resolved modes were investigated using positive matrix factorization (PMF) model.

PM_{10} chemical composition varies by seasons. The highest PM_{10} concentrations are found in the fall with the lowest concentration in the spring. Secondary sulfate and organic matters (1.8 × OC) were the two largest PM_{10} components, accounting for 26–37% and 8–30% of PM mass.

Tri-modal size distributions are found for SO_4^{2-}, NH_4^+ and OC, with mass median aerodynamic diameters (MMADs) of 0.4, 0.7, and 3.8 μm for the condensation, droplet and coarse modes, and a similar width (i.e., standard deviation, σ, ranging 1.32–1.42). The droplet mode is most prominent for SO_4^{2-}, NH_4^+, K^+, OC, and EC. NO_3^- is more prominent in the coarse mode, whereas a single coarse mode is found for Cl^-.

The condensation mode mass is explained of 36% secondary SO_4^{2-} factor, 26% engine exhaust factor, along with 18–19% each for residual oil combustion and coal/biomass burning factors. Eight source factors contribution were in the droplet mode, with from 23% SO_4^{2-} factor, 19% from industrial emissions factor, and 14–16% each for engine exhaust, secondary NO_3^-, and sea salt factor. Approximately, 80% of coarse mode mass is attributed to sea salt and soil factors.

Acknowledgments

The authors wish to acknowledge the financial support of the Environmental Conservation Fund of Hong Kong (7/2009) and the Research Grants Council of the Hong Kong Special Administrative Region (PolyU 152083/14E and PolyU 152090/15E). We thank Professor Tao Wang and his group member of Hong Kong Polytechnic University, Dr. Kinfai Ho of the Chinese University of Hong Kong for their contribution on field study and Hong Kong Environmental Protection Department for providing gaseous data.

References

Andreas, M.O., 1983. Soot carbon and excess fine potassium: long-range transport of combustion-derived aerosols. Science 220, 1148–1151.
Bian, Q., Huang, X.H.H., Yu, J.Z., 2014. One-year observations of size distribution characteristics of major aerosol constituents at a coastal receptor site in Hong Kong — part 1: inorganic ions and oxalate. Atmos. Chem. Phys. 14, 9013–9027.
Cheng, Y.F., Eichler, H., Wiedensohler, A., Heintzenberg, J., Zhang, Y.H., Hu, M., Herrmann, H., Zeng, L.M., Liu, S., Gnauk, T., Brüggemann, E., He, L.Y., 2006. Mixing state of elemental carbon and non-light-absorbing aerosol components derived from in situ particle optical properties at Xinken in Pearl River Delta of China. J. Geophys. Res.-Atmos. 111, D20204.
Cheung, H.-C., Wang, T., Baumann, K., Guo, H., 2005. Influence of regional pollution outflow on the concentrations of fine particulate matter and visibility in the coastal area of southern China. Atmos. Environ. 39, 6463–6474.
Choi, J.C., Lee, M., Chun, Y., Kim, J., Oh, S., 2001. Chemical composition and source signature of spring aerosol in Seoul, Korea. J. Geophys. Res.-Atmos. 106, 18067–18074.
Chow, J.C., Watson, J.G., 1999. Ion Chromatography in Elemental Analysis of Airborne Particles. Elemental Analysis of Airborne Particles. In: Landsberger, S., Creatchman, M. (Eds.), vol. 1. Gordon and Breach Science, Amsterdam, The Netherlands, pp. 97–137 (Chapter: 3, Publisher).
Chow, J.C., Watson, J.G., Lowenthal, D.H., Magliano, K.L., 2005. Loss of PM2.5 nitrate from filter samples in Central California. J. Air Waste Manage. Assoc. 55, 1158–1168.
Chow, J.C., Watson, J.G., Chen, L.-W.A., Chang, M.O., Robinson, N.F., Trimble, D., Kohl, S., 2007. The IMPROVE_A temperature protocol for thermal/optical carbon analysis: maintaining consistency with a long-term database. J. Air Waste Manage. Assoc. 57, 1014–1023.
Chow, J.C., Watson, J.G., Lowenthal, D.H., Magliano, K.L., 2008. Size-resolved aerosol chemical concentrations at rural and urban sites in Central California, USA. Atmos. Res. 90, 243–252.
Chow, J.C., Watson, J.G., Chen, L.W.A., Rice, J., Frank, N.H., 2010a. Quantification of $PM_{2.5}$ organic carbon sampling artifacts in US networks. Atmos. Chem. Phys. 10, 5223–5239.
Chow, J.C., Watson, J.G., Kohl, S., Chen, L.-W.A., Chai, W., 2010b. Measurements and Validation for the 2008/2009 Particulate Matter Study in Hong Kong. Desert Research Institute. NV, Reno, USA.
Chow, J., Watson, J., Robles, J., Wang, X., Chen, L.W.A., Trimble, D., Kohl, S., Tropp, R., Fung, K., 2011. Quality assurance and quality control for thermal/optical analysis of aerosol samples for organic and elemental carbon. Anal. Bioanal. Chem. 401, 3141–3152.
Chow, J., Lowenthal, D., Chen, L.W.A., Wang, X., Watson, J., 2015. Mass reconstruction methods for $PM_{2.5}$: a review. Air Qual. Atmos. Health 8, 243–263.

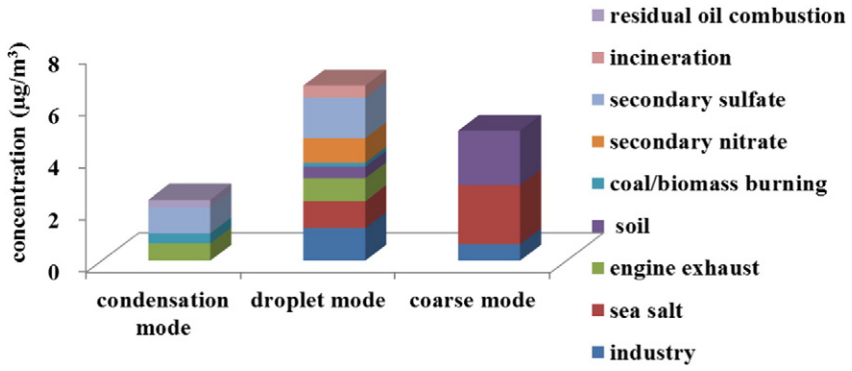

Fig. 9. Source contribution estimates for condensation, droplet, and coarse modes.

Contini, D., Cesari, D., Genga, A., Siciliano, M., Ielpo, P., Guascito, M.R., Conte, M., 2014. Source apportionment of size-segregated atmospheric particles based on the major water-soluble components in Lecce (Italy). Sci. Total Environ. 472, 248–261.
Fujitani, Y., Hasegawa, S., Fushimi, A., Kondo, Y., Tanabe, K., Kobayashi, S., Kobayashi, T., 2006. Collection characteristics of low-pressure impactors with various impaction substrate materials. Atmos. Environ. 40, 3221–3229.
Fung, Y.S., Wong, L.W.Y., 1995. Apportionment of air pollution sources by receptor models in Hong Kong. Atmos. Environ. 29, 2041–2048.
Gao, Y., Lai, S., Lee, S.-C., Yau, P.S., Huang, Y., Cheng, Y., Wang, T., Xu, Z., Yuan, C., Zhang, Y., 2015. Optical properties of size-resolved particles at a Hong Kong urban site during winter. Atmos. Res. 155, 1–12.
Garrido Frenich, A., Martínez Galera, M., Martínez Vidal, J.L., Massart, D.L., Torres-Lapasió, J.R., De Braekeleer, K., Wang, J.-H., Hopke, P.K., 2000. Resolution of multicomponent peaks by orthogonal projection approach, positive matrix factorization and alternating least squares. Anal. Chim. Acta 411, 145–155.
Guo, H., Ding, A.J., So, K.L., Ayoko, G., Li, Y.S., Hung, W.T., 2009. Receptor modeling of source apportionment of Hong Kong aerosols and the implication of urban and regional contribution. Atmos. Environ. 43, 1159–1169.
Guo, S., Hu, M., Wang, Z.B., Slanina, J., Zhao, Y.L., 2010. Size-resolved aerosol water-soluble ionic compositions in the summer of Beijing: implication of regional secondary formation. Atmos. Chem. Phys. 10, 947–959.
Han, J., Moon, K., Lee, S., Kim, Y., Ryu, S., Cliff, S., Yi, S., 2006. Size-resolved source apportionment of ambient particles by positive matrix factorization at Gosan background site in East Asia. Atmos. Chem. Phys. 6, 211–223.
Hand, J., Copeland, D., Day, A., Indresand, D., Malm, W., McDade, C., Moore, C., Pitchford, M., Schichtel, B., Watson, J., 2011. Spatial and seasonal patterns and temporal variability of haze and its constituents in the United States: report V: June 2011. Cooperative Institute for Research in the Atmosphere for the IMPROVE program. Ft. collins, Co.
Hering, S.V., Friedlander, S.K., 1967. 1982. Origins of aerosol sulfur size distributions in the Los Angeles basin. Atmos. Environ. 16, 2647–2656.
Ho, K.F., Lee, S.C., Cao, J.J., Chow, J.C., Watson, J.G., Chan, C.K., 2006. Seasonal variations and mass closure analysis of particulate matter in Hong Kong. Sci. Total Environ. 355, 276–287.
Howell, S.G., Huebert, B.J., 1998. Determining marine aerosol scattering characteristics at ambient humidity from size-resolved chemical composition. J. Geophys. Res.-Atmos. 103, 1391–1404 (1984–2012).
Huang, X.F., Yu, J.Z., 2008. Size distributions of elemental carbon in the atmosphere of a coastal urban area in South China: characteristics, evolution processes, and implications for the mixing state. Atmos. Chem. Phys. 8, 5843–5853.
Huang, Z., Harrison, R.M., Allen, A.G., James, J.D., Tilling, R.M., Yin, J., 2004. Field intercomparison of filter pack and impactor sampling for aerosol nitrate, ammonium, and sulphate at coastal and inland sites. Atmos. Res. 71, 215–232.
Huang, X.-F., Yu, J.Z., He, L.-Y., Hu, M., 2006a. Size distribution characteristics of elemental carbon emitted from Chinese vehicles: results of a tunnel study and atmospheric implications. Environ. Sci. Technol. 40, 5355–5360.
Huang, X.F., Yu, J.Z., He, L.Y., Hu, M., 2006b. Size distribution characteristics of elemental carbon emitted from Chinese vehicles: results of a tunnel study and atmospheric implications. Environ. Sci. Technol. 40, 5355–5360.
Huang, X.F., Yu, J.Z., He, L.Y., Yuan, Z.B., 2006c. Water-soluble organic carbon and oxalate in aerosols at a coastal urban site in China: size distribution characteristics, sources, and formation mechanisms. J. Geophys. Res.-Atmos. 111.
John, W., Wall, S.M., Ondo, J.L., Winklmayr, W., 1990. Modes in the size distributions of atmospheric inorganic aerosol. Atmos. Environ., Part A 24, 2349–2359.
Kadowaki, S., 1986. On the nature of atmospheric oxidation processes of sulfur dioxide to sulfate and of nitrogen dioxide to nitrate on the basis of diurnal variations of sulfate, nitrate, and other pollutants in an urban area. Environ. Sci. Technol. 20, 1249–1253.
Kerminen, V.-M., Wexler, A.S., 1995. Enhanced formation and development of sulfate particles due to marine boundary layer circulation. J. Geophys. Res.-Atmos. 100, 23051–23062.
Khoder, M.I., 2002. Atmospheric conversion of sulfur dioxide to particulate sulfate and nitrogen dioxide to particulate nitrate and gaseous nitric acid in an urban area. Chemosphere 49, 675–684.
Kim, E., Hopke, P.K., Larson, T.V., Covert, D.S., 2003. Analysis of ambient particle size distributions using unmix and positive matrix factorization. Environ. Sci. Technol. 38, 202–209.
Kong, S., Wen, B., Chen, K., Yin, Y., Li, L., Li, Q., Yuan, L., Li, X., Sun, X., 2014. Ion chemistry for atmospheric size-segregated aerosol and depositions at an offshore site of Yangtze River Delta region, China. Atmos. Res. 147–148, 205–226.
Kumar, A., Sarin, M.M., Sudheer, A.K., 2008. Mineral and anthropogenic aerosols in Arabian Sea-atmospheric boundary layer: sources and spatial variability. Atmos. Environ. 42, 5169–5181.
Lan, Z.-J., Chen, D.-L., Li, X., Huang, X.-F., He, L.-Y., Deng, Y.-G., Feng, N., Hu, M., 2011. Modal characteristics of carbonaceous aerosol size distribution in an urban atmosphere of South China. Atmos. Res. 100, 51–60.
Lee, E., Chan, C.K., Paatero, P., 1999. Application of positive matrix factorization in source apportionment of particulate pollutants in Hong Kong. Atmos. Environ. 33, 3201–3212.
Liu, S., Hu, M., Slanina, S., He, L.Y., Niu, Y.W., Bruegemann, E., Gnauk, T., Herrmann, H., 2008. Size distribution and source analysis of ionic compositions of aerosols in polluted periods at Xinken in Pearl River Delta (PRD) of China. Atmos. Environ. 42, 6284–6295.
Louie, P.K.K., Chow, J.C., Chen, L.W.A., Watson, J.G., Leung, G., Sin, D.W.M., 2005. PM2.5 chemical composition in Hong Kong: urban and regional variations. Sci. Total Environ. 338, 267–281.
Malm, W.C., Pitchford, M.L., 1997. Comparison of calculated sulfate scattering efficiencies as estimated from size-resolved particle measurements at three national locations. Atmos. Environ. 31, 1315–1325.
Malm, W.C., Sisler, J.F., Huffman, D., Eldred, R.A., Cahill, T.A., 1994. Spatial and seasonal trends in particle concentration and optical extinction in the United States. J. Geophys. Res. 99, 1347–1370.
Milford, J.B., Davidson, C.I., 1987. The Sizes of Particulate Sulfate aed Nitrate 1B the Atmosphere—A-Review. JAPCA 37, 125–134.
Novakov, T., Corrigan, C.E., 1996. Cloud condensation nucleus activity of the organic component of biomass smoke particles. Geophys. Res. Lett. 23, 2141–2144.
Paatero, P., Tapper, U., 1994. Positive matrix factorization: a non-negative factor model with optimal utilization of error estimates of data values. Environmetrics 5, 111–126.
Penttinen, P., Timonen, K.L., Tiittanen, P., Mirme, A., Ruuskanen, J., Pekkanen, J., 2001. Ultrafine particles in urban air and respiratory health among adult asthmatics. Eur. Respir. J. 17, 428–435.
Plaza, J., Pujadas, M., Gómez-Moreno, F.J., Sánchez, M., Artíñano, B., 2011. Mass size distributions of soluble sulfate, nitrate and ammonium in the Madrid urban aerosol. Atmos. Environ. 45, 4966–4976.
Polissar, A.V., Hopke, P.K., Paatero, P., Malm, W.C., Sisler, J.F., 1998. Atmospheric aerosol over Alaska: 2. elemental composition and sources. J. Geophys. Res.-Atmos. 103, 19045–19057.
Seinfeld, J.H., Pandis, S.N., 2006. Atmospheric Chemistry and Physics: From air Pollution to Climate Change. John Wiley & Sons.
Senaratne, I., Shooter, D., 2004. Elemental composition in source identification of brown haze in Auckland, New Zealand. Atmos. Environ. 38, 3049–3059.
Sisler, J.F., Malm, W., Gebhart, K., Pitchford, M.L., 1996. Spatial and Seasonal Patterns and Long Term Variability of the Composition of the Haze in the United States. Ft. Collins, Co, CIRA (Report ISSN, 0737-5352).
Sloane, C.S., 1983. Optical properties of aerosols—comparison of measurements with model calculations. Atmos. Environ. (1967) 17, 409–416.
Sloane, C.S., Wolff, G.T., 1985. Prediction of ambient light scattering using a physical model responsive to relative humidity: validation with measurements from Detroit. Atmos. Environ. (1967) 19, 669–680.
Sloane, C.S., Watson, J., Chow, J., Pritchett, L., Willard Richards, L., 1991. Size-segregated fine particle measurements by chemical species and their impact on visibility impairment in Denver. Atmos. Environ., Part A 25, 1013–1024.
Tan, J.-H., Duan, J.-C., Ma, Y.-L., Yang, F.-M., Cheng, Y., He, K.-B., Yu, Y.-C., Wang, J.-W., 2014. Source of atmospheric heavy metals in winter in Foshan, China. Sci. Total Environ. 493, 262–270.
Tan, J., Duan, J., Zhen, N., He, K., Hao, J., 2016. Chemical characteristics and source of size-fractionated atmospheric particle in haze episode in Beijing. Atmos. Res. 167, 24–33.
Tang, I.N., 1996. Chemical and size effects of hygroscopic aerosols on light scattering coefficients. J. Geophys. Res.-Atmos. 101, 19245–19250 (1984–2012).
Tsai, J.-H., Lin, J.-H., Yao, Y.-C., Chiang, H.-L., 2012. Size distribution and water soluble ions of ambient particulate matter on episode and non-episode days in Southern Taiwan. Aerosol Air Qual. Res. 12, 263–274.
Wang, T., Guo, H., Blake, D.R., Kwok, Y.H., Simpson, I.J., Li, Y.S., 2005. Measurements of trace gases in the inflow of South China Sea background air and outflow of regional pollution at Tai O, Southern China. J. Atmos. Chem. 52, 295–317.
Wang, X., Wang, T., Pathak, R., Hallquist, M., Gao, X., Nie, W., Xue, L., Gao, J., Gao, R., Zhang, Q., Wang, W., Wang, S., Chai, F., Chen, Y., 2013. Size distributions of aerosol sulfates and nitrates in Beijing during the 2008 Olympic Games: impacts of pollution control measures and regional transport. Adv. Atmos. Sci. 30, 341–353.
Watson, J.G., 2002. Visibility: science and regulation. J. Air Waste Manage. Assoc. 52, 628–713.
Watson, J.G., Chow, J.C., Frazier, C.A., 1999. X-ray fluorescence analysis of ambient air samples. In: Landsberger, S., Creatchman, M., Vo-Dinh, T. (Eds.), Advances in Environmental Industrial and Process Control Technologies: v, 1st ed. Gordon and Breach Science Publishers, Amsterdam, The Netherlands, pp. 67–96.
Watson, J.G., Chow, J.C., Chen, L.W.A., Frank, N.H., 2009. Methods to assess carbonaceous aerosol sampling artifacts for IMPROVE and other long-term networks. J. Air Waste Manage. Assoc. 59, 898–911.
Watson, J.G., Chow, J.C., Lowenthal, D.H., Antony Chen, L.W., Shaw, S., Edgerton, E.S., Blanchard, C.L., 2015. PM2.5 source apportionment with organic markers in the Southeastern Aerosol Research and Characterization (SEARCH) study. J. Air Waste Manage. Assoc. 65, 1104–1118.
Yao, X., Fang, M., Chan, C.K., 2002. Size distributions and formation of dicarboxylic acids in atmospheric particles. Atmos. Environ. 36, 2099–2107.
Yao, X., Lau, A.P.S., Fang, M., Chan, C.K., Hu, M., 2003a. Size distributions and formation of ionic species in atmospheric particulate pollutants in Beijing, China: 1—inorganic ions. Atmos. Environ. 37, 2991–3000.
Yao, X.H., Fang, M., Chan, C.K., 2003b. The size dependence of chloride depletion in fine and coarse sea-salt particles. Atmos. Environ. 37, 743–751.
Yau, P.S., Lee, S.C., Cheng, Y., Huang, Y., Lai, S.C., Xu, X.H., 2013. Contribution of ship emissions to the fine particulate in the community near an international port in Hong Kong. Atmos. Res. 124, 61–72.
Yu, H., Wu, C., Wu, D., Yu, J.Z., 2010. Size distributions of elemental carbon and its contribution to light extinction in urban and rural locations in the Pearl River Delta Region, China. Atmos. Chem. Phys. 10, 5107–5119.
Zhang, R., Jing, J., Tao, J., Hsu, S.C., Wang, G., Cao, J., Lee, C.S.L., Zhu, L., Chen, Z., Zhao, Y., Shen, Z., 2013. Chemical characterization and source apportionment of PM2.5 in Beijing: seasonal perspective. Atmos. Chem. Phys. 13, 7053–7074.
Zhou, S., Wang, T., Wang, Z., Li, W., Xu, Z., Wang, X., Yuan, C., Poon, C.N., Louie, P.K.K., Luk, C.W.Y., Wang, W., 2014. Photochemical evolution of organic aerosols observed in urban plumes from Hong Kong and the Pearl River Delta of China. Atmos. Environ. 88, 219–229.
Zhuang, H., Chan, C.K., Fang, M., Wexler, A.S., 1999a. Formation of nitrate and non-sea-salt sulfate on coarse particles. Atmos. Environ. 33, 4223–4233.
Zhuang, H., Chan, C.K., Fang, M., Wexler, A.S., 1999b. Size distributions of particulate sulfate, nitrate, and ammonium at a coastal site in Hong Kong. Atmos. Environ. 33, 843–853.